Simulation of the Electron Flux into the Main Injector Electron Cloud Retarding Field Analyzer using Vorpal

FERMILAB-PUB-12-584-APC-CD

Paul L. G. Lebrun,* James F. Amundson, and Panagiotis G. Spentzouris
Fermi National Accelerator Laboratory, Illinois, USA

Seth A. Veitzer and Peter Stoltz
Tech-X Corp., Boulder, Colorado, USA

(Dated: October 29, 2012)

We present results from precision simulations of the electron cloud (EC) in the Fermilab Main Injector (MI), focusing on the dynamics of this EC close to the Retarding Field Analyzer (RFA) detectors. Our simulations are based on the Vorpal package. It is found that the presence of a parasitic, weak (few Gauss) magnetic field significantly alters the spatial distribution of electrons in the cloud. The detected flux can easily change by factors of two depending on the location of the RFA. Moreover, the growth rate of the EC is also sensitive to such magnetic field. Therefore, we suggest to (i) upgrade the RFA preamplifier to ≈ 10 MHz bandwidth such that the change in growth rate during a complete MI bunch train can be detected; (ii) install a small solenoid (of ≈ 25 Gauss maximum) to optionally switch off the EC, and thereby cleanly establish the presence of low energy electrons in the pipe; and (iii) design an RFA that can be inserted in a ≈ 0.2 T field, such that an EC signal can be seen in the environment that matters, i.e., in the MI dipoles.

PACS numbers: 29.27.-a
Keywords:

I. MOTIVATION

The electron cloud (EC) phenomenon in high intensity proton storage rings and synchrotrons can limit the performance of such machines (Pivi and Furman [5], Zimmermann [7]). This phenomenon is characterized by an exponential growth of the number of low energy (eV) electrons emitted at the surface of the beam pipe wall. These electrons are then accelerated by the field induced by the passing proton beam, causing more secondary emission when these electrons collide with the beam pipe wall. An essential part of our simulation program is to interpret and guide further experimental developments. More specifically, our focus here is to provide valuable information regarding the interpretation of the data taken with the Retarding Field Analyzer (RFA) (C.Y. Tan [2,3]) at the the Fermilab Main Injector. The non-directional magnetometers located in the vicinity of one of these RFAs have been replaced by a new magnetometer that gives each spatial component of the field. The data from this new magnetometer, shown in Figure 1, has been used in our 3D Vorpal simulation. As we will show, we were able to confirm the sensitivity of this detection technique to small parasitic magnetic fields. This note describes the simulation method and our results as well as giving suggestions on how to verify some of our Vorpal-based predictions.

II. THE VORPAL SETUP

The configuration of the Fermilab Main Injector (MI) RFA has been previously described by C.Y. Tan [2,3]); here we give only the relevant details about Vorpal simulations of the RFA. Vorpal (See C. Nieter [1]), is an object-oriented C++ framework for 1D, 2D and 3D parallel electromagnetic and electrostatic simulation of fully relativistic charged fluids and particles on a structured grid. Vorpal includes 2nd-order accurate physical models of particle/wall interactions, secondary electron emission, space charge effects, as well as mechanisms for measuring time histories of all physically-relevant quantities.

A 3D code is required for this application, as the arbitrary direction of the parasitic field breaks both the left/right longitudinal symmetry and the azimuthal symmetry – there are no preferred directions in this problem. Also note that the magnetic field created by the beam current, peaking at about 11 A (approximating the bunch shape as square, one ns duration, pulse of 7.0×10^{10} protons per bunch), produces a magnetic field at ≈ 1 cm from the beam that

*Electronic address: lebrun@fnal.gov

Operated by Fermi Research Alliance, LLC under Contract No. De-AC02-07CH11359 with the United States Department of Energy.

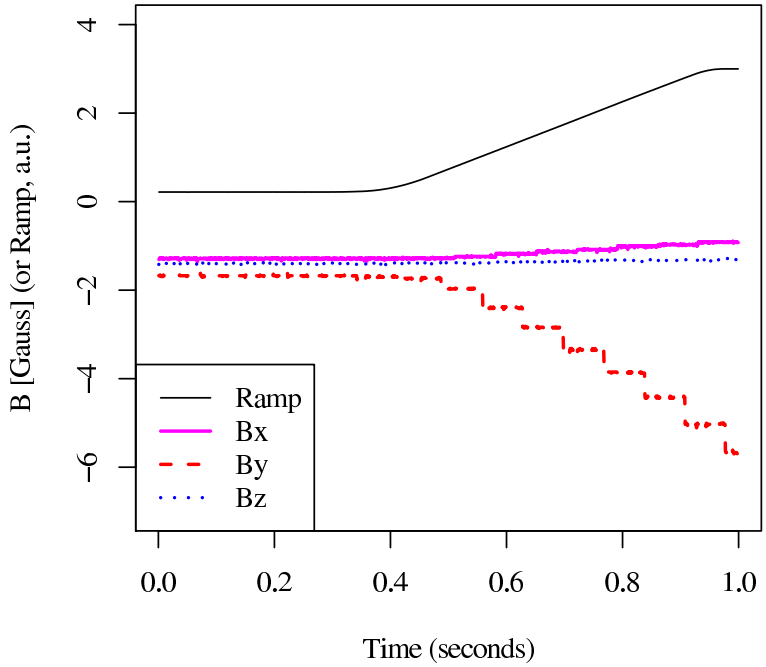

FIG. 1: The parasitic magnetic field as a function of time during the Main Injector ramp (shown in black).

is comparable to this parasitic field. The use of Vorpal in this context has been previously documented by Lebrun et al. [4]. The length of the physical region where the EC is simulated is 50 cm long, which is much larger than the diameter of the pipe (six inches) and the size of the RFA aperture. The secondary emission yield (SEY) is assumed to be 2.2, as the beam pipe is made of "un-scrubbed" stainless steel.[9]

A detailed numerical model of the RFA, with its exact physical geometry, including the field shaping grid, in presence of the proton beam current has not yet been implemented. Such a detailed simulation is outside of the scope of this work. However, the simpler simulation presented here already provides interesting results. The entrance of the device has been simulated at two distinct levels. First, the SEY at these entrance slots has been set to zero, such that no electrons are directly produced within the direct aperture of the device. Second, Vorpal electron files are periodically generated, allowing us to make arbitrary 6D phase space selection of the relevant macro-particles, and if need be, to compute the electron flux in the device above a fixed secondary electron energy.

This is a nearly non-relativistic problem, where radiation from the electrons is negligible, and where no external radio frequency fields are present. Thus EM radiation can be altogether ignored. However, the field due to the space charge fields in the EC itself are important, and they do change in the time commensurate with the passage of the proton beam. The corresponding electric field has a broad frequency spectrum[10], some of it above the frequency cutoff of the beam pipe. Thus, our Vorpal simulation includes "perfectly matching layers" that simulate the open boundary condition of the upstream and downstream ends of the pipe.

Finally, as in any particle-in-cell (PIC) code, one must be careful to use the appropriate grid size to avoid asymmetries due to inappropriate cell size. In our case, for a transverse grid size of 3.4 mm, spikes in the electron density appeared at azimuthal angles $\phi = 0$, $\pm\pi$ and $\pm\pi/2$, when stray magnetic fields were turned off and the beam was exactly centered in the cylindrical beam pipe. That is, no asymmetry at all in ϕ would be expected. However, since the electron density varies rapidly in the region within a few mm from the wall, such a spurious asymmetry, due to artifacts of the PIC algorithms, is not at all surprising. Reducing the transverse cell size to 1.7 mm mostly fixed the problem, leaving a residual ϕ asymmetry of less then two percent at the beginning of the simulation and 0.5% after a few proton bunches, when the statistics start to accumulate due to the onset of the multipacting phenomena.

III. SIMULATION RESULTS

The goal of this particular simulation is to investigate the reliability of the EC densities measured by the RFA in the presence of systematic uncertainties. More specifically, as the RFA detects only a small fraction of the electrons in the pipe, assumptions about the uniformity of the EC density must be assessed. The first systematic uncertainty

could be due to a beam displacement with respect to the center of the beam pipe. Indeed, if the beam is displaced vertically with respect to the beam pipe walls, a ϕ anisotropy appears quite early in the multipacting process, at the onset of the exponential growth of the cloud, as shown in Figure 2. This anisotropy gradually disappears as the electrons have a chance to migrate away from the beam region.

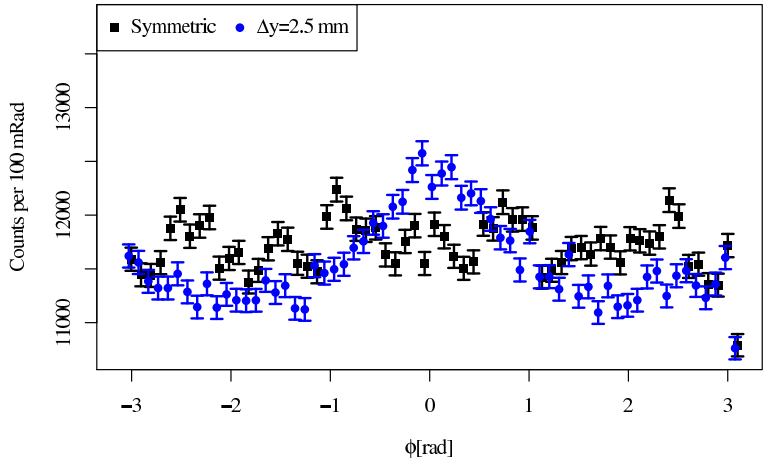

FIG. 2: Distribution of the electrons' azimuthal angle ϕ with respect to the vertical direction. Macro-electrons located near the upstream/downstream edges of the pipe have been rejected. The electron density is also smooth along the beam axis. This is 128 ns after the first proton bunch. No cuts have been placed on the electron energy.

The presence of stray magnetic field reconfigures the cloud as well, as shown in Figure 3. At all times during the bunch train, the induced asymmetry in ϕ due off-axis magnetic fields is larger than that induced by a beam offset. As expected, this asymmetry depends on the electron energy in a non-trivial way; the 3D acceleration of electrons due to the stray magnetic field, the proton bunch and the space charge of the cloud all depend on both time and space. The asymmetry in ϕ persists at later times, and is more pronounced for more energetic electrons, as shown in Figure 4. The scatter in the data, which is significantly greater than the expected statistical fluctuations in the number of macro-particles in the simulation, is simply due to the fact that the EC density is sampled every 7.3 ns while the EC is strongly perturbed at every bunch crossing, i.e., every 18.8 ns.

The growth time of the cloud is also a non-trivial probe of the dynamics, starting from a rarefied cloud due to gas ionization to the phase where the self space charge forces dominate the motion between proton bunches. The electron density averaged over the physical region ($\pm 75.$ cm of the pipe) is shown in Figure 5. The stray magnetic field allows for a slightly more efficient transport and acceleration of the electrons from the beam region to the walls. For the relevant case, where the stray magnetic field is present, the EC is in a nearly steady state after about 30 proton bunch crossings. The density reaches then $2.4\,10^{12}$ electrons per m^3, corresponding to ratio of the electron to proton linear density of about 50%[11]. The EC density above a kinetic energy of 20 (40) eV is about $5.\,10^{11}$ ($2.3\,10^{11}$) electrons per m^3, respectively.

From this simulated data, the flux into the RFA can be readily estimated. The ensemble of macro-electrons that hits the wall in the vicinity of the RFA has been saved so that a post-simulation analysis can be performed on electrons that might enter the RFA. If integrated over the duration of the passing of a few proton bunches, the exact longitudinal position of such macro-electrons do not matter, allowing us to consider a bigger sample of electrons than the one covering the limited extent of the RFA (about one inch). The distributions of the transverse coordinates are also fairly uniform across the limited aperture of the RFA. The momentum distributions are those estimated by Vorpal. These macro-electrons have been propagated through both the entrance slits of the RFA and the static electric field located between the grid and the collector. The electric field maps are based on a detailed simulation using the SIMION C.Y. Tan [2], SIMION [6] package. The simulated current on the collector is shown in Figure 6. The slits and the grid are assumed to be completely passive, in the sense that possible field emissions from edges are neglected, as are any possible secondary emissions. The bias voltage on the RFA's grid was set to 20 Volts.

On the time scale of the passing of a few proton bunches, the current is proportional to the density, and saturates at $4.6\,\mu A$. On shorter time scales, both density and predicted RFA current fluctuate by quite a bit more then the expected statistical uncertainty on the number of macro-particles. This reflects the broad frequency content of the electromagnetic fields present in the cloud.

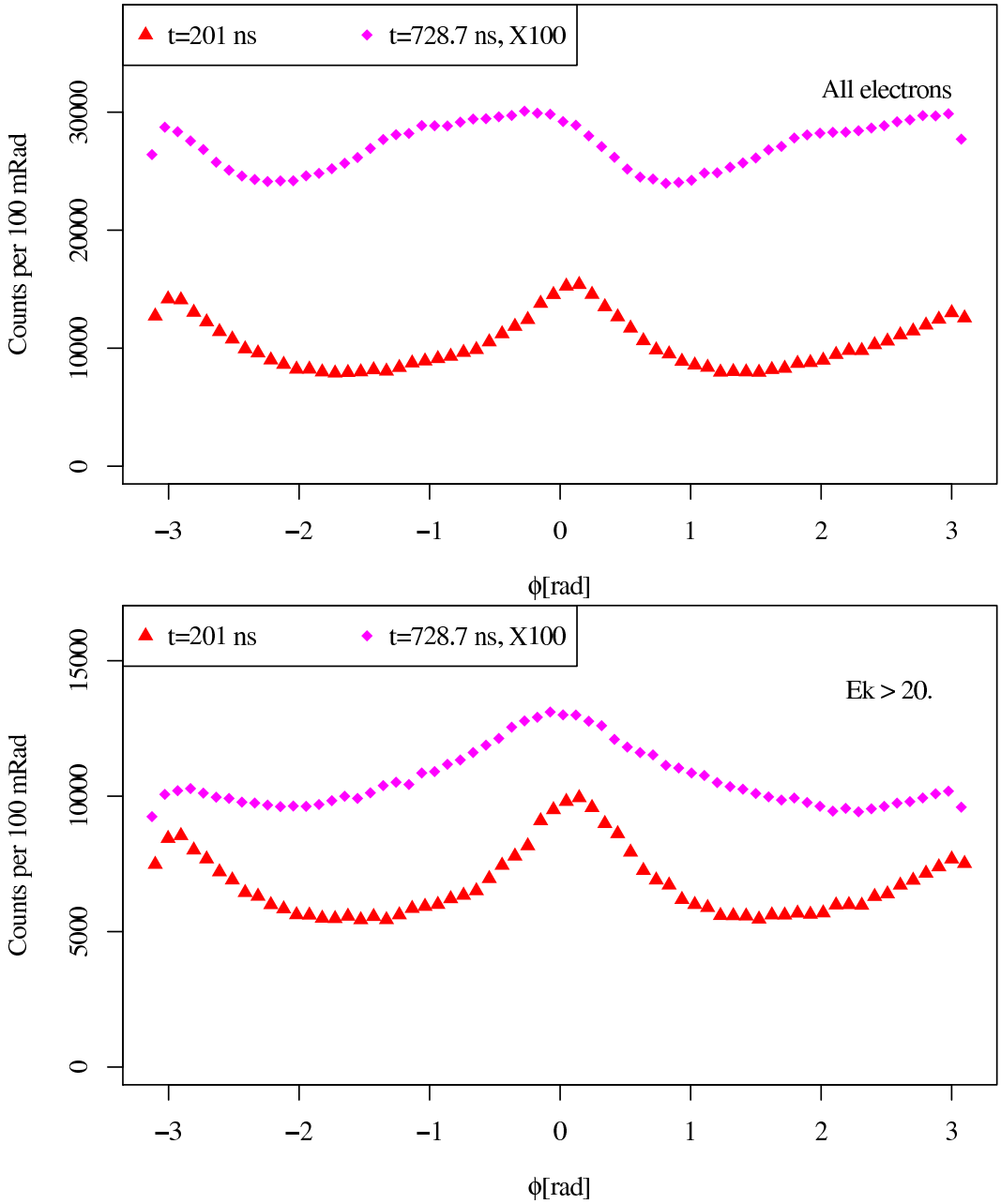

FIG. 3: Distribution of the same electron's azimuthal angle ϕ, taken 201 ns after the first bunch in the booster batch, and 28 bunches later (at $t = 727$ ns), for three cuts on the kinetic energy of the macro-electrons (0., 20); top and bottom plots respectively). The cloud is growing at $t \approx 201$ ns (characteristic time of ≈ 60 ns), while the growth is much slower $t \approx 727$ ns, when space charge has become important.

IV. CONCLUSIONS

A simulation of the electron cloud near the Main Injector RFA has been done. The presence of a stray magnetic field as low as $\approx$ 3.5 Gauss affects both the growth time and the geometry of the EC. Noting that real RFA devices can only measure the integrated flux above $\approx$ 20 Volt, over many turns, as the response time of the preamplifier is no better than 1.0/3.0 kHz, many of our predictions can not yet be verified. Nevertheless, it is clear that the current configuration of the stray magnetic field boosts the yield of electrons that the RFA collects. This excess yield should persist up the ramp, as the vertical component of the stray field increases along with the Main Injector ramp. This is not what has been observed Zwaska [8]. To resolve this discrepancy and better understand the performance of the

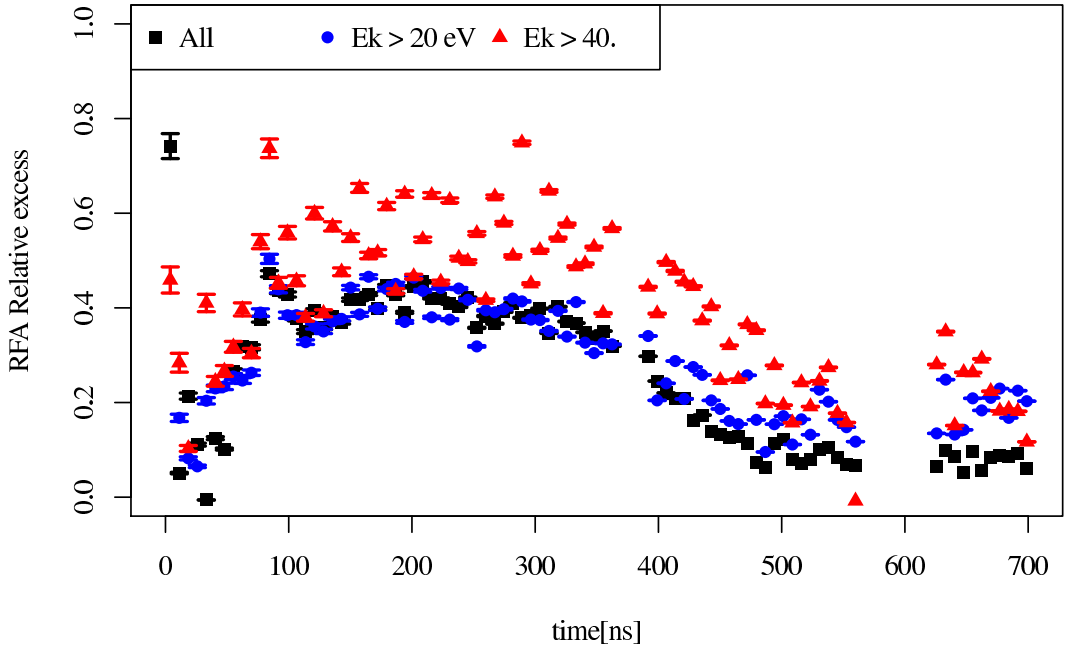

FIG. 4: Evolution of the ϕ asymmetry, defined as the integrated density within the ϕ RFA aperture relative to the average density, for macro-particles a few mm away from the entrance of the RFA, over about 30 proton bunches, for three values of the threshold cut on the macro electron kinetic energy.

device, we suggest to install an extinguishing solenoid over $\approx \pm 50$ cm of the RFA. Such a field would deflect all electrons produced in the center of the pipe away from the beam pipe wall and from the RFA. The second suggested upgrade is to improve the bandwidth of the electronics that measure the RFA current, such that the near extinction of the cloud in the beam abort gap can be detected. Ultimately, ≈ 5 ns timing could be achieved with a more involved detector, where these electrons produce photons off a scintillating material, and such photons are detected with a fast image amplifier, a multi-anode PMTs, or if cost a real concern, a single PMT.

V. ACKNOWLEDGMENT

The RFA field map was prepared and delivered to us by Chen Yang Tan. We greatly appreciate his contribution. Numerous discussions with Bob Zwaska were very productive.

This work was supported by the United States Department of Energy under contract DE-AC02-07CH11359 and the ComPASS project funded through the Scientific Discovery through Advanced Computing program in the DOE Office of High Energy Physics. This research used resources of the National Energy Research Scientific Computing Center, which is supported by the Office of Science of the U.S. Department of Energy under Contract No. DE-AC02-05CH11231. This research used resources of the Argonne Leadership Computing Facility at Argonne National Laboratory, which is supported by the Office of Science of the U.S. Department of Energy under contract DE-AC02-06CH11357.

1. J. R. Cary C. Nieter. Vorpal: a versatile plasma simulation code. *J. Comp. Phys.*, 196, 2004.
2. R. Zwaska C.Y. Tan, K.L. Duel. An improved retarding field analyzer for electroncloud studies. `http://accelconf.web.cern.ch/AccelConf/PAC2009/papers/th5rfp041.pdf`, 2009.
3. R. Zwaska C.Y. Tan, M. Backfish. The ecloud measurement setup in the main injector. `http://www-spires.slac.stanford.edu/spires/find/hep/www?r=fermilab-conf-10-508-ad`, 2010.
4. P. Lebrun et al. Simulation of the electron cloud in the fermilab main injector. `http://inspirebeta.net/record/913965`, 2011.
5. M. T. Pivi and M. A. Furman. Electron cloud development in the proton storage ring and in the spallation neutron source. *Phys. Rev. ST Accel. Beams*, 6, 2003.

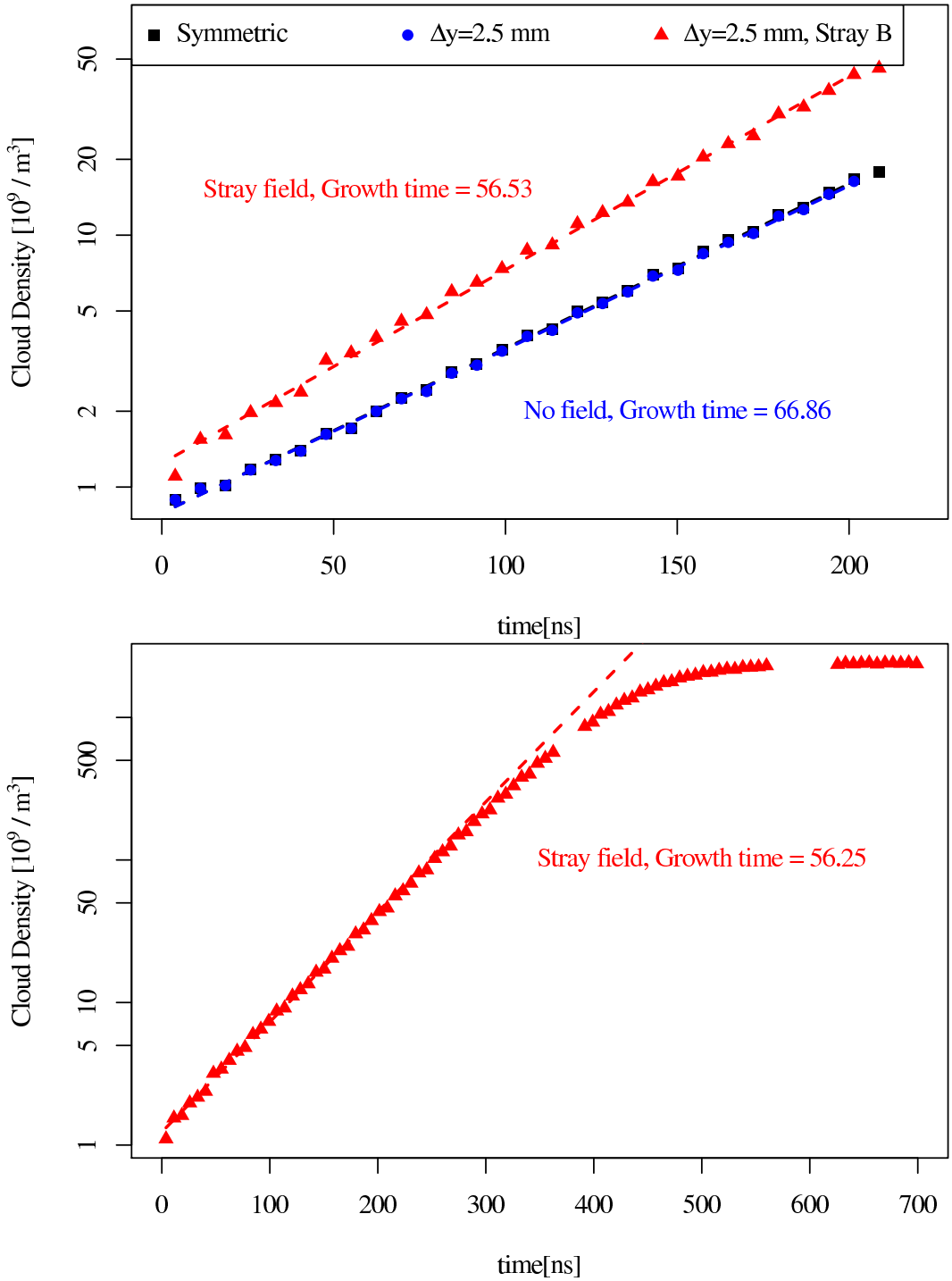

FIG. 5: The EC density as a function of time after the first bunch crossing, for the various cases described in the text.

6. SIMION. Industry standard charged particle optics simulation software. `http://simion.com`, 2008.
7. F. Zimmermann. Review of single bunch instabilities driven by an electron cloud. *Phys. Rev. ST Accel. Beams*, 7, 2004.
8. R. Zwaska. Electron cloud experiments at fermilab: Formation and mitigation. `http://lss.fnal.gov/archive/2011/conf/fermilab-conf-11-081-apc.pdf`, 2011.
9. This large SEY value is probably realistic after the pipe has been exposed to air, then pumped down, as is the case in the beginning of a typical run. At the beginning of a run, the RFA signal tends to be relatively high, then, probably due to scrubbing, the signal decreases over time, in a matter of days to weeks.
10. See, for instance, Figure 11 in ref Lebrun et al. [4]

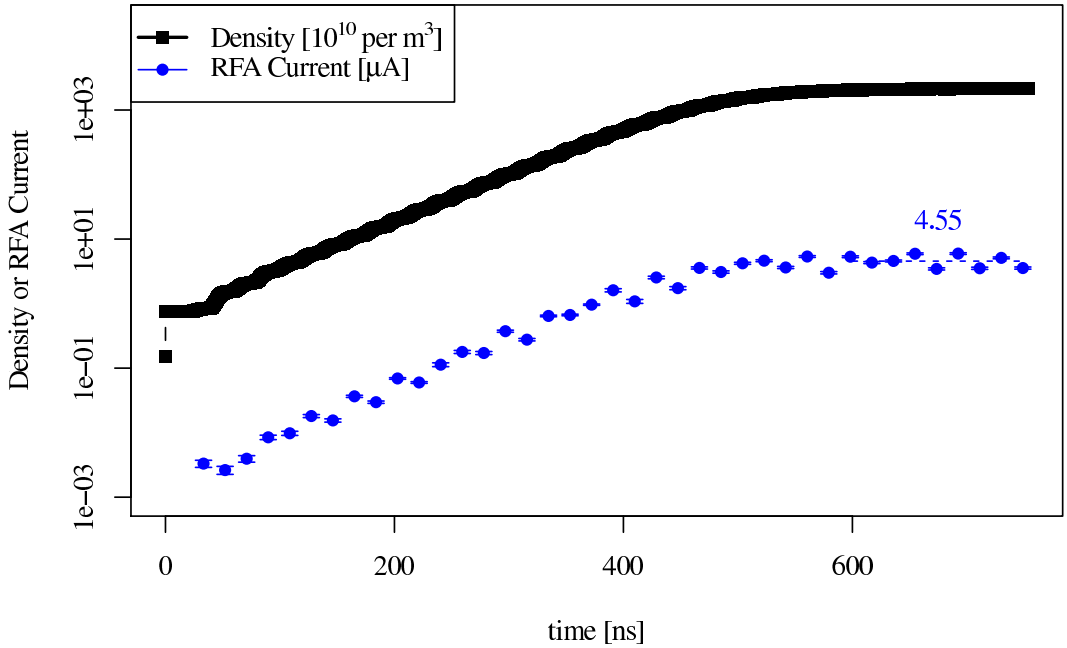

FIG. 6: The simulated electron current measured by the RFA and the cloud density. The stray magnetic field is taken from 1.

11. The linear proton density is measured when the bunches are present in the pipe, over an effective length of $\sqrt{2\pi}\,\sigma$, or $8.4\,10^{10}$ electrons per meter, for $7\,10^{10}$ protons per bunch